Supplementary Information

Sprayable Anti-Adhesive Hydrogel for Peritoneal Macrophage Scavenging in Post-Surgical Applications

Table of content

Name	Abbreviation	Host	Reactivity	Dilution	Company	Catalog #
Human/Mouse/Rat iNOS Antibody	Anti-iNOS	Mouse	Mouse, Rat, Human	200:1	Novus Biologicals	MAB9502
Anti-Mannose Receptor antibody	Anti-CD206	Rabbit	Mouse, Rat, Human	200:1	Abcam	ab64693
Arginase1 Polyclonal Antibody	Anti-Arg1	Rabbit	Mouse, Rat, Human	200:1	Invitrogen	PA5-85267
APC/Fire™ 750 anti-mouse F4/80 Antibody	APC/Fire™ 750 anti-F4/80	Rat	Mouse	50:1	BioLegend	123151
Pacific Blue™ anti-mouse F4/80 Antibody	Pacific Blue™ anti-F4/80	Rat	Mouse	50:1	BioLegend	123123
CD11b Monoclonal Antibody (M1/70), Alexa Fluor™ 488, eBioscience™	Alexa Fluor™ 488 anti-CD11b	Rat	Mouse	50:1	Invitrogen	53-0112-82

Supplementary Table 1: Information of antibodies used in the study.

Sample	S (%)	C (%)	H (%)	N (%)	Degree of sulfation (%)	Molecular weight (kDa)
HA	Not detected	31.90 ± 2.23	4.84 ± 0.26	2.60 ± 0.19	0	1356.55 ± 153.80
sHA	10.71 ± 0.12	22.50 ± 1.78	3.48 ± 0.10	1.62 ± 0.25	62.63 ± 4.28	82.88 ± 5.98

Supplementary Table 2: Identification of degree of substitution through elemental analysis and molecular weight through gel permeation chromatography.

Nozzle diameter (mm)	Flow rate (mL min^{-1})	Air pressure (kPa)	Distance from target (cm)
1	10	150	5

Supplementary Table 3: Identification of degree of substitution through elemental analysis and molecular weight through gel permeation chromatography.

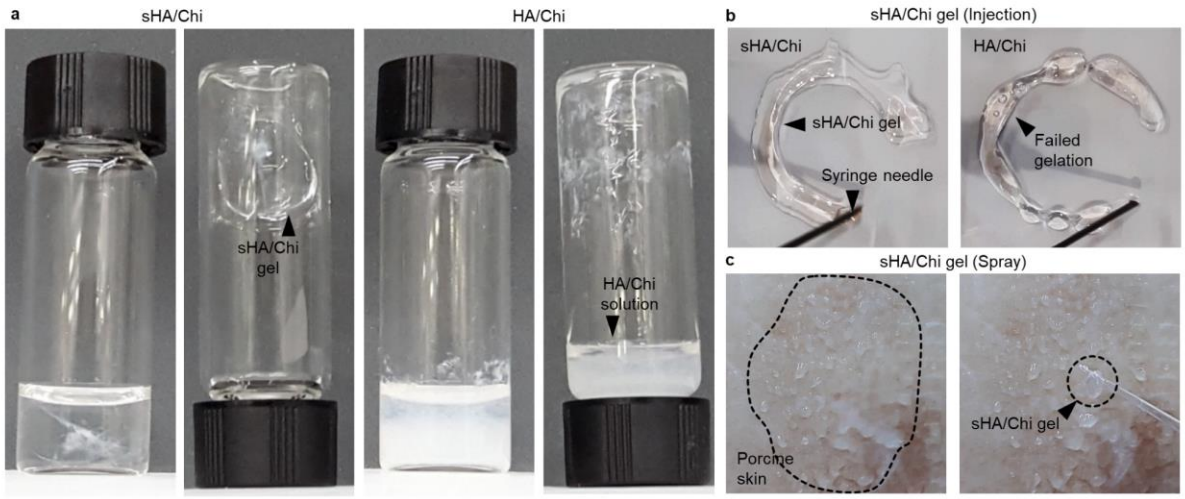

Supplementary Fig. 1: In situ gelation of sHA/CS mixture. **a** Representative images of the inverted vial test for the sHA/CS mixture and HA/CS mixture. **b** Representative images of the injectability test for the sHA/CS mixture and HA/CS mixture, with red ink added to the mixtures for visualization. **c** Representative images of the sprayability test of the sHA/CS mixure on porcine skin.

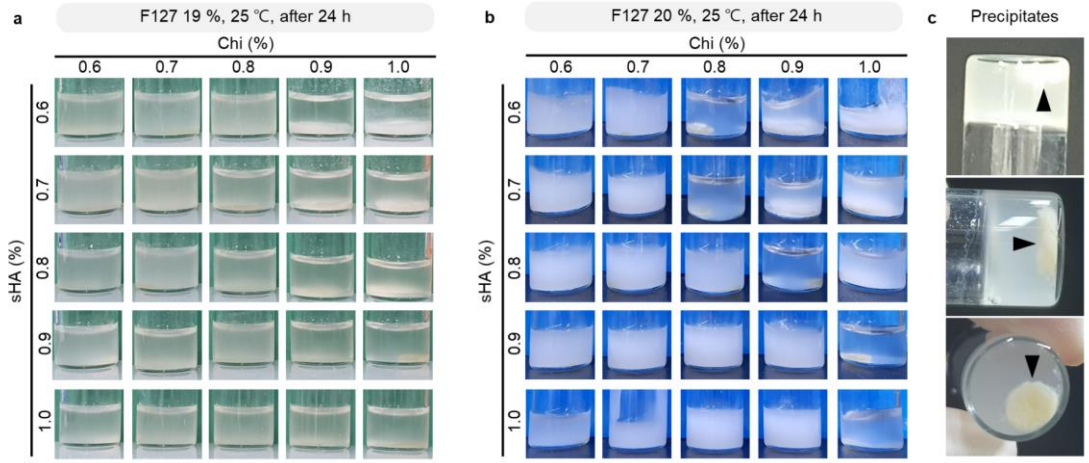

Supplementary Fig. 2: Precepitation of polyelectrolyte complex between sHA and CS in various sHACSF formulations. **a** Precipitation of sHACSF (F127 19 %) after 24 h of incubation. **b** Precipitation of sHACSF (F127 20 %) after 24 h of incubation. **c** Representative images of the precipitation of sHACSF (sHA 0.8 %, CS 1.0 %, and F127 20 %).

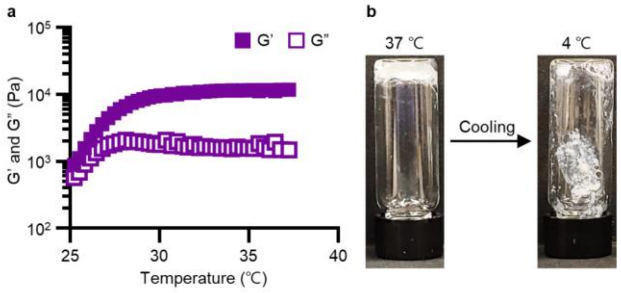

Supplementary Fig. 3: Thermogelation of sHAChiF. **a** Temperature sweep test of sHAChiF performed from 25 ℃ to 37 ℃. **b** Inverted vial test of sHAChiF from 37 ℃ to 4 ℃.

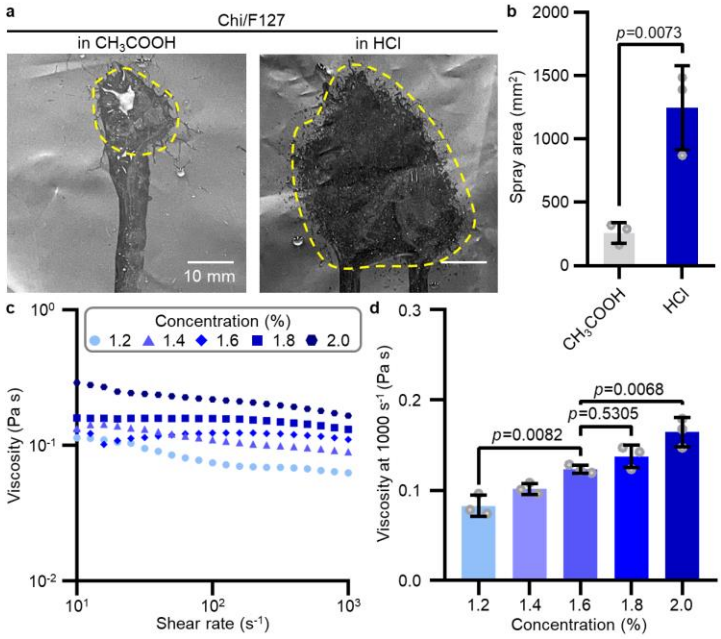

Supplementary Fig. 4: Screening of CS concentration for sprayable CS/F127 mixture. **a** Representative images of the sprayability test of the CS/F127 mixtures dissolved with different acids (CH_3COOH and HCl). **b** Quantificaiton of the sprayed area for the CS/F127 mixtures with different acids (CH_3COOH and HCl). **c** Concentration-dependent behavior of viscosity in the CS/F127 mixtures. **d** Quantification of viscosity at a shear stress of 1000 s^{-1} for the CS/F127 mixtures. Data are shown as mean ± SD (n = 3 independent samples in **a, b**; n = 3 independent samples in **c, d**). Two-tailed unpaired t-test was used for statistical analysis of **b**. One-way ANOVA with Tukey post-hoc test was used for statistical analysis of **d**. Source data are provided as a Source Data file.

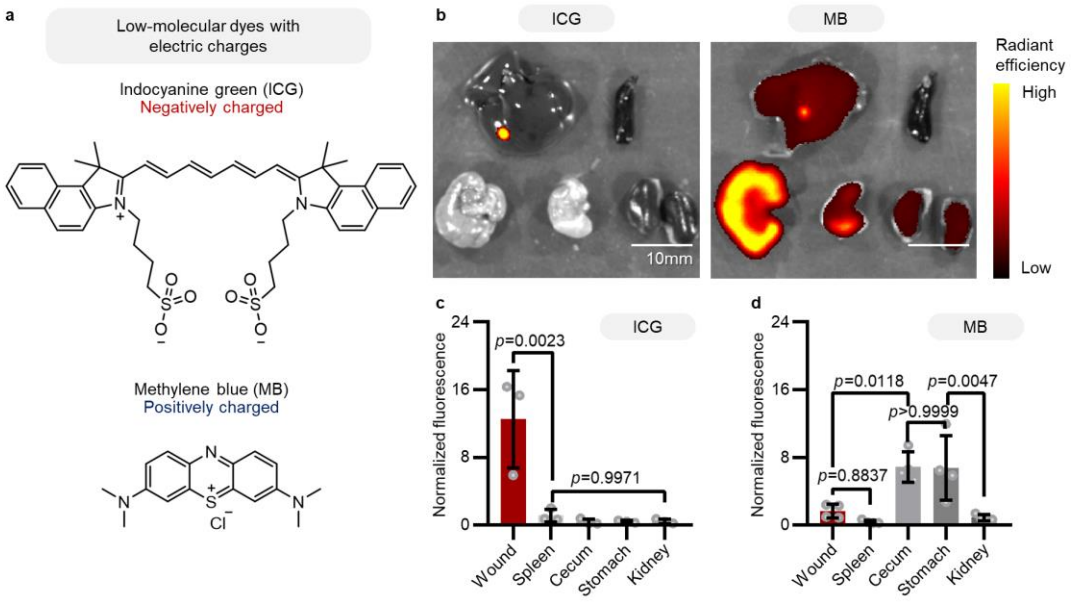

Supplementary Fig. 5: Differential organ-distribution patterns between anionic (ICG) and cationic (MB) molecules in a mouse hepatic thermal wound model. **a** Schematic illustration of the ICG and MB. **b** Representative IVIS images of various mouse organs in the mouse hepatic thermal wound model treated with ICG and MB after thermal injury (Scale bar = 10 mm). **c** Quantification of ICG and MB fluorescence, normalized by fluorescence from the normal liver. Data are shown as mean ± SD (n = 4 independent samples in **b-d**). One-way ANOVA with Tukey post-hoc test was used for statistical analysis of **c, d**. Source data are provided as a Source Data file.

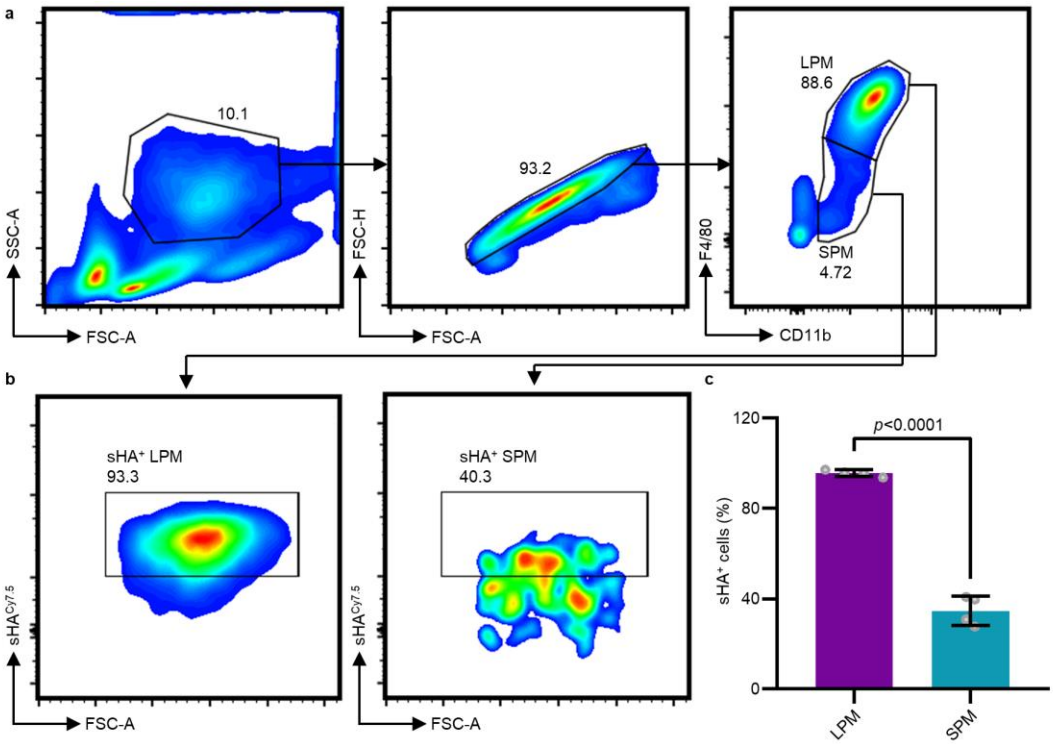

Supplementary Fig. 6: Flow cytometry analysis for sHA$^+$ LPM quantification. **a** Flow cytometry gating strategy used to define LPM and SPM. **b** Flow cytometry gated on sHA$^+$ peritoneal macropahges (LPM and SPM). **c** Quantification of sHA$^+$ peritoneal macrophages (LPM and SPM). Data are shown as mean ± SD (n = 4 independent samples in **a-c**). Two-tailed unpaired t-test was used for statistical analysis of **c**. Source data are provided as a Source Data file.

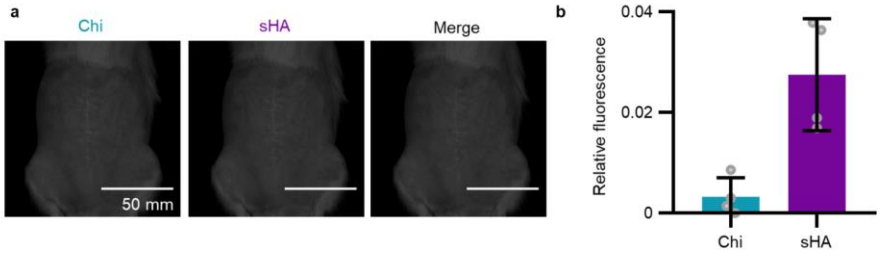

Supplementary Fig. 7: Long-term in vivo retention of sHAChiF in rat ischemic button model. **a** Representative IVIS images of fluorescence by Chi$^{Cy5.5}$ and sHA$^{Cy7.5}$ in dual-sprayable hydrogels, 6 month after surgery (Scale bar = 50 mm). **b** Fluorescence intensity of Chi$^{Cy5.5}$ and sHA$^{Cy7.5}$ in sHAChiF, 6 month after surgery, normalized by fluorescence at d 0. Data are shown as mean ± SD (n = 4 independent samples in **a, b**). Source data are provided as a Source Data file.

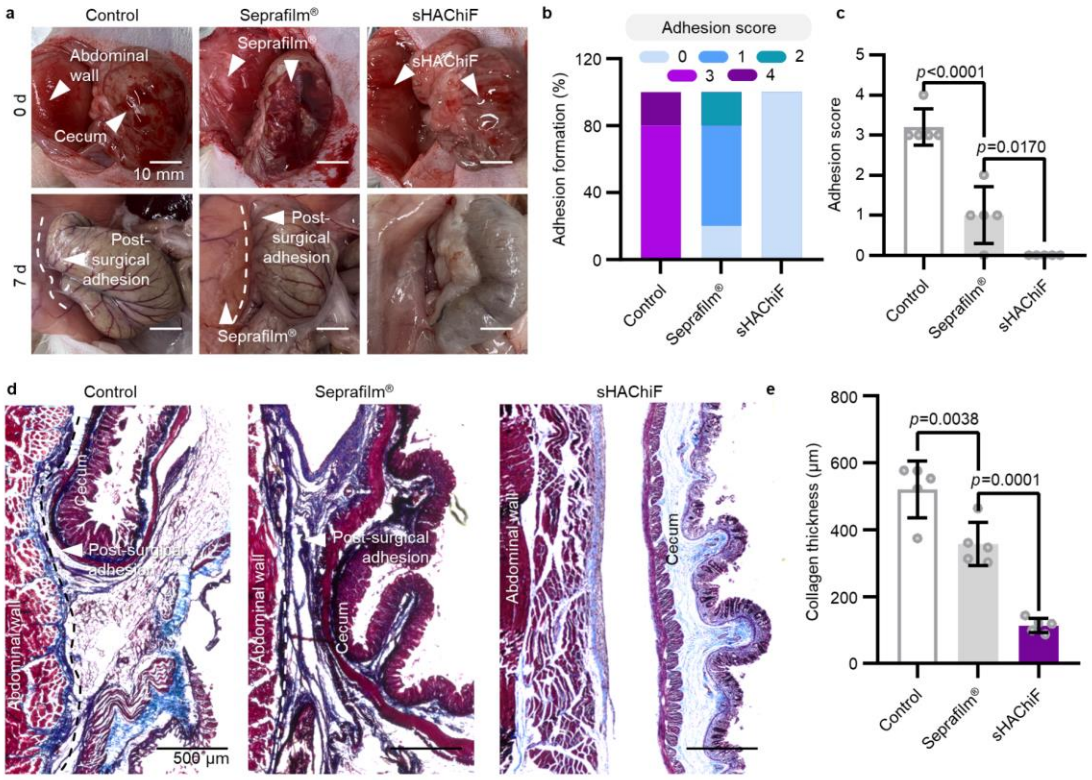

Supplementary Fig. 8: Prevention of peritoneal adhesion in rat cecal abrasion model using sHAChiF. **a** Representative images of rat cecal abrasion model on d 0 and d 7 after surgery (Scale bar = 10 mm). **b** Adhesion formation rates with adhesion scores of sHAChiF per rat. **c** Quantification of the adhesion scores of dual-sprayable hydrogels. **d** Representative Masson's trichrome staining images of adhesive tissues on d 7 after surgery (Scale bar = 500 μm). **e** Quantification of collagen thickness of adhesive tissues on d 7 after surgery. Data are shown as mean ± SD (n = 5 independent samples in **a-e**). One-way ANOVA with Tukey post-hoc test was used for statistical analysis of **c**, **e**. Source data are provided as a Source Data file.

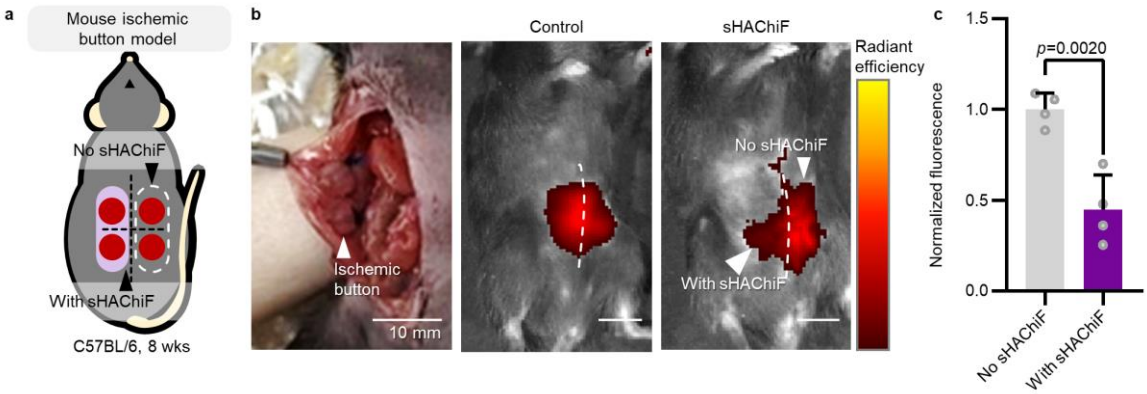

Supplementary Fig. 9: In vivo IVIS imaging of inflammation by ProSense®750 FAST. **a** Schematic illustration of mouse ischemic button model with sHACSF treatment on the half of the buttons. **b** Representative images of IVIS imaging of the C57BL/6 mouse 4 d after operation

(Scale bar = 10 mm). **c** Quantification of the fluorescence level of the ProSense®750 FAST normalized by the area without sHACSF treatment. Data are shown as mean ± SD (n = 4 independent samples in **a-c**). Two-tailed unpaired t-test was used for statistical analysis of **c**. Source data are provided as a Source Data file. Image was created using PowerPoint.

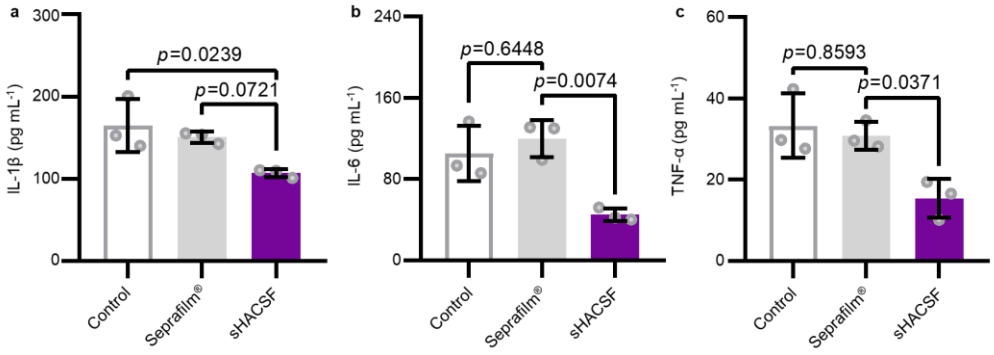

Supplementary Fig. 10: Quantification of pro-inflammatory cytokines in rat ischemic button model on d 7 after surgery. **a** IL-1β. **b** IL-6. **c** TNF-α. Data are shown as mean ± SD (n = 4 independent samples in **a-c**). Two-tailed unpaired t-test was used for statistical analysis of **a-c**. Source data are provided as a Source Data file.